Simulating and Communicating Outcomes in Disaster Management Situations

Michal Lichter[1], A.Yair Grinberger[2] and Daniel Felsenstein[3]

[1] mlichter@gmail.com Department of Geography, Hebrew University of Jerusalem Mount Scopus, 91900 ISRAEL

[2] asherya.grinberger@mail.huji.ac.il Department of Geography, Hebrew University of Jerusalem Mount Scopus, 91900 ISRAEL

[3] msdfels@mscc.huji.ac.il Department of Geography, Hebrew University of Jerusalem Mount Scopus, 91900 ISRAEL

Abstract

An important but overlooked component of disaster rmanagment is raising the awareness and preparedness of potential stakeholders. We show how recent advances in agent based modeling and geo-information analytics can be combined to this effect. Using a dynamic simulation model, we estimate the long run outcomes of two very different urban disasters with severe consequences: an earthquake and a missile attack. These differ in terms of duration, intensity, permanance and focal points. These hypothetical shocks are simulated for the downtown area of Jerusalem. Outcomes are compared in terms of their potential for disaster mitigation. The spatial and temporal dynamics of the simulation yield rich outputs. Web-based mapping is used to visualize these results and communicate risk to policy makers, planners and the informed public. The components and design of this application are described. Implications for participatory disaster management and planning are discussed.

Keywords: Agent Based Modeling, Web GIS, Spatial Computing, Hazard Managenet,

1.Introduction

Communicating the likely outcomes of catastophic events to potential stakeholders is an integral part of disaster management. Building community resilience is as much about improving accessibility to information and arousing awareness of hazards, as it is about engaging engineering solutions. However, this aspect of post-disaster management has been less investigated as it deals with longer term, less tangible outcomes. Short-term protective fixes for hazards are always easier to quantify, visualize and promote. In the case of coastal flooding for example, defensive mechanisms can be easily illustrated and animated while the disequilibrating effects on population and land use are harder to convey.

The situation is further comfounded by the fact that technology for potentially conveying these outcomes is moving ahead faster than the ability to generate applications. This means that much potential information that could be made available lies dormant for lack of suitable means of communication. In addition, the frequency and intensity of natural disaster events is becoming ever more extreme and less predictable. This serves to underscore the importance of a long-term perspective over a short-term hazard response. Aside from the immdediate needs for flood evacuation, disease prevention, building reconstruction and the like, disaster management needs to also be concerned with raising awareness and preparedness through communicating plausible outcomes.

This paper illustrates how some of the analytic tools of geo-informatics can be harnessed for both generating and conveying outcomes in disaster management. For generating disaster outcomes, we used agent-based simulation. We utilize dynamic web mapping as the vehicle for communicating these outcomes. The next section discusses some of the uses of web-GIS for disaster management. This is followed by a concise description of the analytic modeling framework in Section 3. The simulation results are presented in section 4 where emphasis is placed on the very different outcomes implied by each disaster. In section 5 we present the web platform for communicating these outcomes and discuss its features. Some of the technical features of the design of the platform including data formats and ancillary functionalities are described in section 6. Finally, we conclude with some implications for public participation in disaster management arising from the increasing transparency of methods and outcomes.

2. Web Mapping for Disaster Management

Web GIS has been heralded as a key component in hazard management and vulnerability assessment [1]. It extends desktop GIS capabilities to an internet environment and thus encourages the development of applications that are accessible, dynamic and interactive. In this respect, it releases disaster managers from the tasks of data collection and map generation and allows them to focus on visualization and analysis. As maps are an intuitive and user-friendly medium for communicating risk [2], is is not suprising that the development of web-based mapping has been conceived as a central axis in incorporating public participation in disaster

management. Little *et al* [3]for example, show how web-based geovisualization tools can both encourage stakeholder involvement and public input into emergency management. The result is a framework that goes beyond improving disaster response and can contribute to the wider organizational realms of training, awareness enhancement and team building.

Many examples exist in which web mapping has been utilized in emergency management. For example, Hagemeier-Klose and Wagner [4] evaluate the use of web mapping services in communicating flood risk and Kwan and Lee [5]analyze the potential use of real-time 3D GIS in the case of terror attacks. In fact, web mapping has raised its public profile through a series of natural and man-made disasters starting with the WTC attack on New York in 2001 and progressing through the ravages of Hurricane Katrina in New Orleans (2005), the Haiti and Christchurch earthquakes in 2010 and 2011, the Tokohu earthquake and tsunami (2011) and Superstorm Sandy (2012).

It should be noted that the collective and participatory mapping that these catastrophic events encourage (crowdsourcing, volunteered information, map mashups etc) challenges the conventional information chain [6]. While web mapping is proclaimed as the ultimate democratizer that delivers information, empowers the public and reduces the digital divide, caution needs to be taken to avoid methodological pitfalls. Web-based information allows for immediate change in spatial resolution. This can encourage miss-use with respect to scale and issues of ecological fallacy. In addition, the ease in which data overlays can be performed can lead to suggestive but spurious correlations. Thus while web-based platforms for disaster management are here to stay, care needs to be invested in their execution and design. They need to deliver outcomes in a seamless and non-technical fashion and these outcomes needs to have been generated in a plausible manner. It is to these two issues that we now turn.

3 Disaster Simulation Framework

We illustrate how geo-information can be generated by using an agent-based (AB) framework to simulate the long-term consequences of a disaster. The value of AB models in this context lies in their ability to create high-resolution representations of the urban environment. The long-term indirect effects of an event are reflected in the behavioral responses of the agents. The outcomes of the disaster can be tied to local, place-specific circumstances. This frees disaster management from the constraints imposed by coarse administrative borders. Additionally AB models can represent dynamics at high levels of temporal resolution. Therefore, the AB framework has been readily applied in the context of natural disaster scenarios such as flooding, fires, and earthquakes [7–11].

AB models are based upon three elements: the environment, the agents and a set of rules guiding agent-agent and agent-environment interactions [12]. The latter may be defined within the model based on social, economic and spatial decision rules. The first two however are exogenous starting conditions of the simulation. As spatial socio-economic and urban data is usually available at aggregates such as census tracts, agent-level data must be generated synthetically. Here we use data disaggregation techniques to create 'big' spatial data in which census tract-level socio-economic values are synthetically distributed over buildings, households and individuals (see Figure 1). The allocation algorithm preserves aggregate census tract-level values. The resulting database is used to represent the starting conditions upon which supply and demand dynamics following a disaster are simulated. These procedures are used to evaluate the long term effects of two scenarios: an earthquake and a missile attack both simulated on the same area in downtown Jerusalem, Israel.

Figure 1: The Analytic Framework
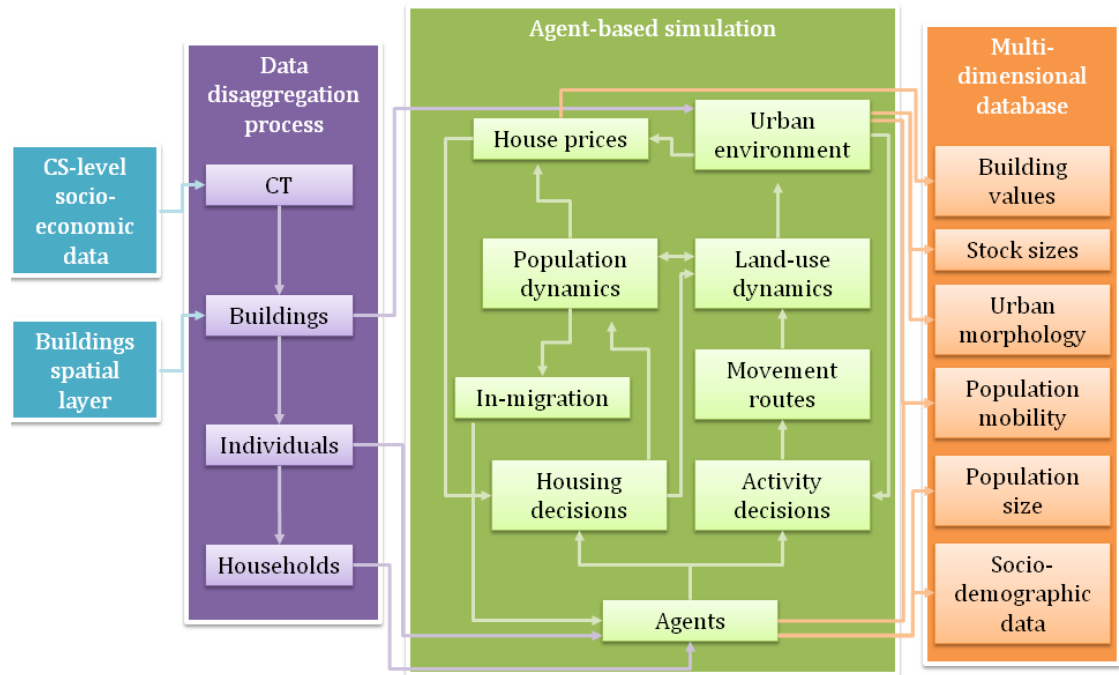
3.1. Spatial context

The simulation is applied to the Jerusalem city center, a mixed-use area including two major commercial centers (the Mahaneh Yehuda enclosed market and the CBD), a number of other commercial and public-use venues and many low-rise residential building (see Figure 2). Three major traffic arteries traverse the area: Agripas St. and Jaffa St. (light-railway route) running north-west to south-east and King George St. running north-south. The area comprises 22,243 residents, 717 residential buildings (243Th sqm), 119 commercial buildings (505Th sqm) and 179 governmental/public buildings (420Th sqm). The occurrence of both scenarios in the area is probable. It is situated 30 km north-west of the active Dead Sea fault[1] and was a focal point for many types of terror attacks over the years, including missile attacks in the summer of 2014.

---

[1] Although the area is relatively seismically stable most of the buildings in this part of the city were constructed before earthquake-related building codes were enforced. This makes them prone to damage in such a scenario[13].

Figure 2: the study area

Legend
Streets Buildings ■ Residential ■ Commercial ■ Public/Governmental

600 300 0 600 Meters

1 – CBD, 2 – Machaneh Yehuda Market, 3 – Jaffa St., 4 – Agripas St., 5 – King George St.

3.2. Generating high-resolution urban data

The literature offers a number of data generation techniques such as population gridding [14], areal interpolation [15], dasymetric representation [16,17] and proportional iterative fitting [18,19]. The method we use here is more in line with the technique used by Harper and Mayhew [20,21]. We combine administrative data available at a coarse spatial level and a detailed buildings GIS layer in order to create spatial representations of individuals and households within buildings and allocate synthetic socio-economic values to them. This involves two stages of disaggregation and one stage of clustering. We use an allocation algorithm to disaggregate from census tracts (CTs) to buildings and from buildings to individuals. We then cluster individuals into households (see Figure 1). At each stage, the dataset is populated with the following values:

- Buildings: land-use, floor-space, number of floors, building values, number of households.
- Households: number of members, earnings, car ownership
- Individuals: household membership, disability, participation in the work force, employment sector, age group, workplace location.

The sources of the data used in this process are the 2008 Israeli Census (for households, individuals and earnings, disability, age, labor force participation and employment by sector), a GPS-survey (for workplace location), National Tax Authority data (residential property value per meter) and capital stock estimates [22].

6

Socio-economic values are allocated to buildings in the first stage in proportion to their floor-space. See Lichter and Felsenstein [23] for a full articulation of the allocation method. As equation 1 illustrates for population size, individual buildings values are calculated by multiplying CT-level densities with buildings-level floor-space:

$$Pop_b = fs_b * \frac{Pop_c}{fs_c}$$

(1)

where *Pop* is population size, *fs* is floor-space, *b* is individual building and *c* is census tract.

Floor-space is calculated according to aerial footprint and height in meters, assuming a floor-height of 5m for residential buildings and 7m for non-residential buildings. These figures were derived by comparing the calculated sum total of floor-space over all buildings by use with total national built floor-space. This proportional allocation process necessarily entails a loss of data due to the division of integers (e.g. population) by fractions (e.g. floor-space). The SQL-based allocation algorithm compensates for this by adjusting the floating point figures rounding threshold for each variable separately. In this manner, the algorithm verifies that CT control totals are met.

At the second stage, each of the individuals is given a unique id that is tied to a specific building and is located at a random location within the building. Next, demographic values (e.g. age, disability, workforce participation) are allocated to individuals so that the entire set of residents within a building represents the distribution of socio-economic variables within it. This distribution corresponds to CT distribution from the previous stage. Finally, individuals within a building are clustered into heterogeneous households. These represent a "traditional household" including both adults and children when possible. The clustering algorithm iterates through individuals and aims to create new household entities which are not identical but are closely similar in terms of age representation. Each household has a unique id, is assigned to a building, and individuals are assigned to it. This process results in a high-resolution big spatial database that includes accurate synthetic representations of 7,354,200 individuals allocated to 771,226 residential buildings (out of 1,075,904 buildings).

3.3. Agent-based simulation dynamics

The synthetic big database is used to characterize the starting conditions of the urban simulation in terms of both environment and agents. In accordance with agent-based modeling, the dynamics of the city are characterized 'bottom-up'. The individual actions of atomic units accumulate as aggregate changes. Households and their members are defined as agents. Their movements through buildings over the road network (representing the environment) over both diurnal and long-term temporal scales leads to environmental change (see Figure 1). The model is implemented within the Repast Simphony 2.0 modeling platform [24]. Each model iteration reflects one day in the urban setting in which agent behavior affects land-use, urban

morphology, capital stock values and population dynamics. The model has been fully described in Grinberger, Lichter and Felsenstein [11].

The behavior of agents revolves around two location decisions – residential location choice made at the household level and individual-level activity decisions. These decisions are based on a combination of constraints (such as budget constraint) and preferences (such as segregative residential tendencies). Preferences reflect a mix of behavioral assumptions – satisficing behavior [25], residential segregation [26], and risk evasiveness. Equation 2 shows an example of such a decision process in the case of residential location:

$$(2) \quad h_{hh} = b_j \Rightarrow \left[\frac{I_{hh}}{3} > HP_j \right] * \left[k_{hh} > \frac{\Phi\left(\frac{\bar{I}_b - \bar{I}_h}{I_{\sigma_h}} \right) + \Phi\left(\frac{\bar{A}_b - \bar{A}_h}{A_{\sigma_h}} \right)}{2} \right] = 1$$

where: h is home location for household hh, b is a building considered as new residence place, *[x]* is a binary expression where 1 if x is true and 0 otherwise, *HP* is monthly cost of living in building j, k is a randomly drawn preference value for the household, *Φ(x)* is the cumulative normal distribution value for x, $\bar{A},\bar{I}$ are building-level average age and income respectively and A_σ, I_σ are standard deviation values for age and income in a building.

In the above equation, the constraint is a budget constraint. The randomly drawn preferences reflect segregative behavior by representing limited tolerance to changes in the demographic nature of the residential neighborhood. Similarly, activity decisions are based on land-use suitability and attractiveness in relation to random preferences. Attractiveness is related to the nature of the environment of the location, distance to current location (which is weighted by the mobility profile of the individual) and floor-space volume. In both decision processes, the first location to satisfy both constraints and preferences is selected in according with satisficing behavior. Number of activities per day is set for each agent according to its mobility profile (age, disability, household car ownership) and employment profile (work force participation, workplace location). Residential mobility is motivated either by exogenous migration probabilities (intra- and inter-urban) or by changes to the environment (land-use change or destruction by disaster). In-migration is also taken into account where the number of potential new households in each iteration is dependent upon an in-migration/out-migration ratio and proportional to the number of idle dwelling spaces.

Supply side interactions are also simulated by conceptualizing different spatial units – CTs, buildings and residential units – as environmentally sensitive entities within a top-down environmental influence procedure (see Figure 1). This process is expressed by changes in land-use patterns and residential units' monthly (rental) prices. Land-uses changes are based on the ratio of floor-space volume to local average traffic loads. We assume that higher volume traffic reflects more revenue from visits (represented by traffic) and greater commercial activity. Low ratio values (high traffic loads in relation to floor-space volume) encourage commercial activity at

the expense of residential supply, while high values make the success of commercial activity less probable[2]. These land-use changes affect house prices, along with changes in supply (number of residential buildings in a CT) and demand (the population size of the CT). Changes to these elements lead to changes in average house prices per meter in the CT. Rising service levels (number of non-residential units) drive up prices and in line with standard economic theory, prices will drop with increase in supply or decrease in demand. CT-level changes trickle down to the level of the individual building proportionate to floor-space volume. In addition, building values are adjusted according to their accessibility to non-residential (i.e. service) functions. Greater accessibility makes a building more valuable. Finally, the value of each residential unit within a building is calculated, assuming uniform values within a building. Values are transformed into monthly housing costs in accordance with the population's willingness-to-pay (represented by the budget constraint in eq. 2).

3.4 Simulated scenarios

We simulate two very different scenarios (Table 1). The first relates to multiple missile attacks. These represent long term continuous, low level attrition of the urban system. The attacks are random in space, time and quantity (magnitude) and there is no single focus of the event. The second scenario is an earthquake. This delivers a catastrophic one-time shock to the urban system and has a defined focus (aftershocks not withstanding). Disaster management in both cases relates to the effects on the urban system in terms of speed to recovery, population and land use change and shifts in urban morphology.

Table 1: Characteristics of Scenarios Simulated

Scenario	Scenario Duration	Effects	Event Dynamics	Scale	Number of Event Foci
Multiple Missile Attack	Long term	Temporary	Diffuse	Citywide	Many
Earthquake	Long term	Permanent	Focused	Citywide	One

Differences between the scenarios are formulated in relation to their temporal extent, intensities, direct and indirect effects. Both the first missile attack and the earthquake occur at day 50 (i.e. the 50th simulation iteration) in order to afford a 'run-in' period for the urban system to stabilize. While the earthquake shock occurs only once, the missile-attacks continue to appear until the simulation ends. The focal center of the shock is determined randomly to avoid place-based bias.

The earthquake is simulated as spreading outwards from the epicenter with declining intensity. The direct physical effect of this shock is manifested through the collapse of buildings. This effect is probabilistic in nature. The chance of a building being damaged is proportional to its distance from the epicenter and its height. The

---

[2] The logistic probability of land-use change is based on the standardized cumulative exponential distribution values of floor-space and traffic loads in order to avoid inflation of small commercial uses and deflation of large land uses.

road nearest to a collapsed building is blocked and remains so until the building is restored. The restoration period is proportional to floor-space area.

The missile attack is simulated as a series of multiple local shocks appearing every day and varying in number from 0 to 10. If a missile hits a road, it remains blocked for that iteration. If a building is hit, there is a 5 percent probability of serious damage which results in the same physical effect as building collapse in the earthquake scenario. In addition to this effect, missile hits impact decision making processes. The accumulation of hits in a single place makes it less attractive as a residential location (reflecting risk-evasiveness), inducing out-migration and reducing in-migration. This is formalized in the behavior of residents. If their close neighborhood (50 meters radius) is hit more than 3 times over the preceding 30 iterations, they are given a 20 percent probability of relocating. Such buildings have a zero chance of attracting new residents. Activity location decisions are also affected as agents avoid choosing destinations that were hit over the course of the current day. Exogenous shocks therefore directly affect urban dynamics via physical changes (destruction of buildings and disruption to movement) and psychological effects (risk evasiveness). Due to the model dynamics, these direct effects lead to a second round of indirect effects.

4 Simulation Outcomes

The results of the simulations include time-series data at high-level spatial resolution. They relate to changes in capital stock and population size, building values, urban morphology and functionality. The richness of the outcomes facilitates analysis of urban development at multiple scales as well as across different scenarios. This section presents examples for macro and micro analysis and comparisons that unveil the main processes of change. These results relate to 25 simulations per scenario where each simulation comprises of 1010 simulated days. The results reported are the simulation averages.

4.1. Macro Trends

Table 2 presents a macro comparison of event effects in the two scenarios. We observe the tendency of key variables to return to pre-shock values and converge over time (over different values). Variables are considered convergent (i.e. reach equilibrium) if they show no significant change over the last 50 iterations or more. The values in Table 2 indicate the day at which on average the last significant change was registered until the end of the simulation.

Population and residential stock variables show similar behavior in the two scenarios in regard to regaining pre-event values. It seems that both types of shocks induce an out-flow of migration which includes more wealthy households. This leads to a slightly reduced and cheaper housing stock. Other variables point to striking differences between the scenarios. First, the immense growth of non-residential stock in the earthquake scenario is replaced by a reduction in size in the missile attack. Moreover, convergence over time is rarely achieved in the latter, while it frequently occurs in the former. These results may be attributed to the nature of the shocks. The missile attacks call for continuous adaptation in face of an on-going event. This

erodes reorganization ability that may be more attainable in the case of a one-time
shock such as an earthquake.

Table 2: Recovery of the Urban System by Simulated Scenario

Parameter	Variable	Earthquake			Missile Attack		
		Average final change (% of pre-shock value)	Frequency of equilibrium (out of 25 simulations)	Average duration to achieve equilibrium (days)	Average final change (% of pre-shock value)	Frequency of equilibrium (out of 25 simulations)	Average duration to achieve equilibrium (days)
Population	Population	67.85	24	397	70.39	3	944
	Average Income	50.53	11	950	50.62	6	954
Residential stock	Residential Stock Size (# buildings)	88.34	25	332	93.30	15	948
	Average Residential Value	96.12	22	677	90.93	7	951
Non-residential stock	Non-Residential Stock Size (# buildings)	142.43	23	670	73.55	4	948
	Average Non-Residential Value	78.61	25	385	89.45	12	926

4.2. Micro Scale Change

Figure 3 presents micro-scale results relating to the different population and
land-use dynamics resulting from the simulated disasters. In this figure, buildings are
characterized at each point in time in terms of the most frequent land-use and the
average Social Vulnerability Index (SVI) of resident households over the
simulations[3]. The SVI relates to demographic characteristics which may enhance or
constrain a household's adaptation capabilities.

---

[3] Following Lichter and Felsenstein (2012), SVI is defined as:

$$SVI_{hh} = 0.5I_{hh} - 0.2A_{hh} + 0.1Car_{hh} - 0.2Dis_{hh}$$

where: *hh* is a household, *I* is monthly income, *A* is average age, *Car* is car ownership, *Dis* is % of
members with disability. All values are standardized.

Figure 3: Changes in land-use and population demographics by building at discrete time points.

Flat (2D) buildings are of non-residential use – grey for vacant, blue for commercial and pink for public/governmental. 3D buildings are residential, where both height and color represent average SVI scores (height represents absolute values) by quantiles – red colors signifying lower scores (high vulnerability) and green higher (low vulnerability).

The strong direct impact of the earthquake leads to immediate consequences. Population is forced to relocate and the initial east-west divide between more and less vulnerable populations (Figure 3, t=50) is fractured (Figure 3, t=100). In contrast, the missile attacks do not create such an accentuated result. The same process of dispersal and re-concentration only appears after damage has accumulated over time (Figure 3, t=1000). This is because the effects on accessibility caused by physical destruction lead to indirect effects on the land-use system. As traffic disperses due to the inaccessibility of some roads, new commercial functions may develop in areas which attract more traffic at the expense of existing commercial venues located near previously busy roads. As traffic is constantly diverted by the continual flow of

12

shocks in the missile scenario, new commercial functions struggle to survive. Accordingly, commercial activity goes into slow and protracted decline as evidenced by the succession of commercial venues becoming vacant along King George St. and in the north-east corner of the study area (Figure 3, t=1000).

On the other hand, in the earthquake scenario decline is accelerated. This enables a stabilization of traffic patterns, around new commercial centers that have succeeded to reorganize. As new functions attract more traffic, an agglomerative process occurs. The new clusters of commercial activity appearing in the areas to the south-west and north-east of the market (Figure 3, t=1000) indicate such a process. Once commercial activity rejuvenates and land-uses patterns become fixed, fluctuations in house prices decrease and the population is able to re-organize. This process is visibly less prominent but can be detected as some of the less vulnerable clusters seem to grow in strength, such as the one south of the market (Figure 3, t=1000). The continuous fluctuations in traffic patterns and in the land-use system under the missile scenario require agents to constantly adapt and disturb any attempt to achieve stability. This attrition effect is associated with constant low-grade shocks.

These contradicting micro-spatial patterns of re-organization versus decay explain the propensity of the system to reach stability in each of the scenarios, as reported in Table 2. Thus, while low-resolution spatial analysis may be useful in identifying patterns of aggregate change, utilizing the spatio-temporal richness of the data allows for insights regarding the causes of such patterns. As can be seen from the level of complexity in Figure 3, it is not easy to communicate these results, especially if both time and space are visualized at high-resolutions.

5. Communicating Outcomes

Traditionally, research outputs are communicated through scientific publications and reports. These are limited in the amount of textual and visual information they contain. These constraints are compounded as the sophistication and volume of outputs increases. Furthermore, public participation in planning and decision-making is gaining increased currency [27,28]. The new consumers of information invariably do not have access to traditional sources of scientific information generating a need for communicating spatial information to professionals and the public alike in a comprehensible and intuitive manner.

Communication of complex and information intensive research results to end-users from wide-ranging backgrounds is a challenging task. With the increase in sophistication, volume and complexity of modeling urban dynamics, and as computing power and big data grow exponentially, this challenge is compounded. Web-based cartographic spatial and temporal visualization technologies can function as a bridge between the research environment in which outputs are generated and the user. We develop a web-based application that serves as a means to communicate outputs generated using an agent-based simulation model to potential end-users, such as urban engineers and evacuation planners. Communicating spatial information in this way helps to increase transparency and opens the door for public awareness and

participation in planning processes post disaster. Our application allows the user to browse through four types of spatial and non-spatial visualization techniques.

5.1 Map comparison panel

In this visualization the user can view four different maps of four different dynamically changing variables in the aftermath of a disaster (missile attack or earthquake): building value, vulnerability index, household income and mobility ratio. The maps are not static but rather can be animated to display a sequence of time lapse portrails of each variable. Each map contains "shots" in space and time of the variables from before the event (t+0) to the time of the event (t+50) to three years after the event (t+1000) in time steps of 50 days. The animated maps of each variable are presented in two formats from which the user can choose. The first is a discrete vector building layer format which displays the change in variable values over time through a change in building color. With a mouse-click on each building, the user can trigger a popup window with all the properties attached to the building (Figure 4). The second format is a heatmap – this is a continuous surface draped over the study site which portrays high and low concentrations of a phenomenon using hot and cold colors. Areas where a certain variable displays high values, such as building values or mobility ratios, will be displayed in red. Areas with low values are displayed in blue. This enables the user to easily identify spatial trends and configurations, dynamically adjusting with the zoom level of the map. It does not however, allow value extraction by a click of the mouse. Both formats allow the user to animate the maps by clicking on the "play" button to automatically animate the maps over time or use a slider to manually change the a maps time steps.

Figure 4: The map comparison panels displaying vector based discrete buildings (a) and contentious heatmap surface (b) for building value (upper left in each panel of four maps), vulnerability index (upper right), household income (lower left) and mobility ratio
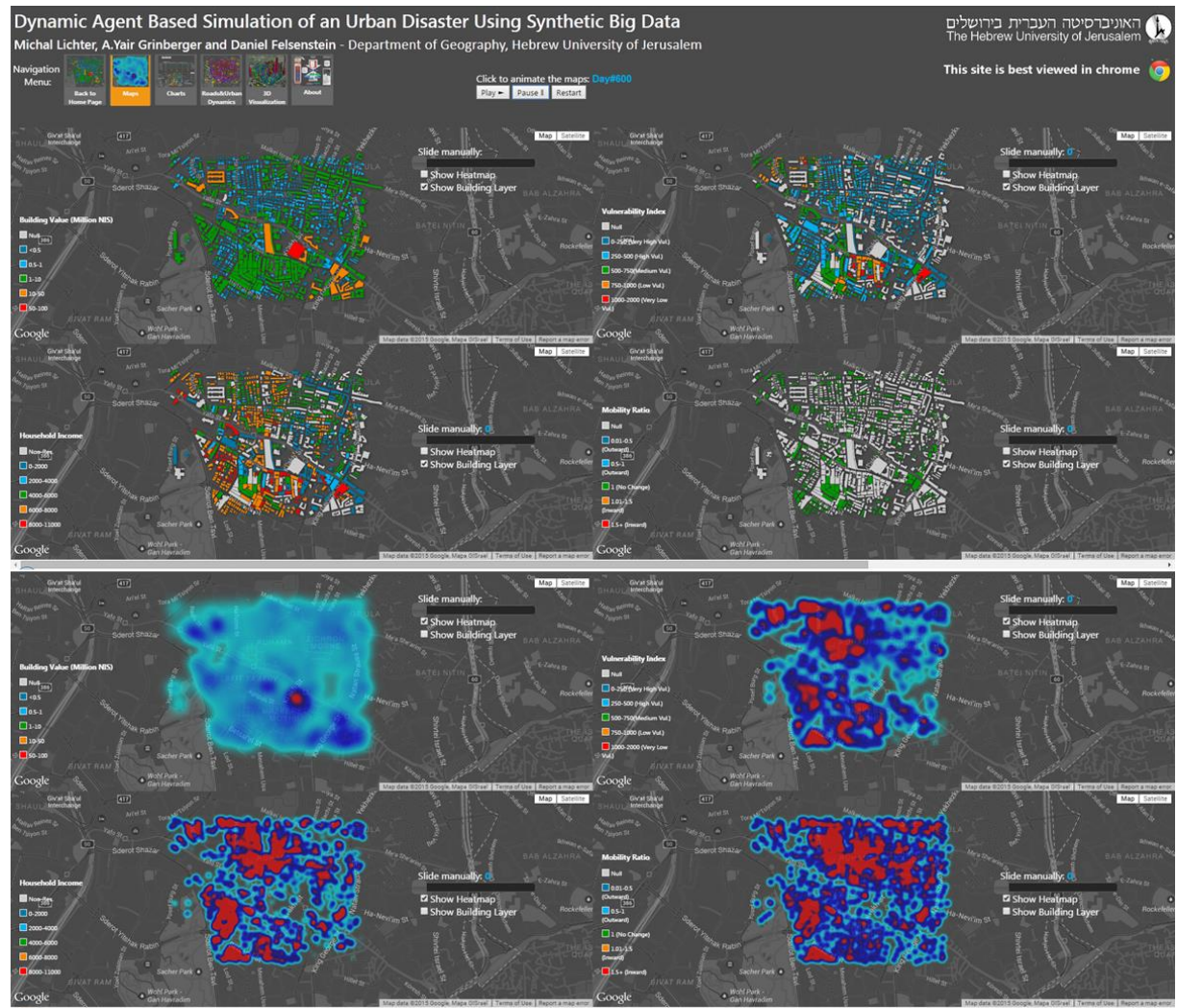
5.2 Dynamic Graphs panel

In this panel, change in parameters is charted over dynamic-queryable graphs (Figure 5). For example, variables relating to population dynamics such as the number of inhabitants in the area and their monthly earnings at each point in time are displayed over the earnings of new in-migrants. This shows the increase in total poulation accompanied by a drop in the total earnings in the study area over the entire three year period post-earthquake. Specifically, the high variance in household income of in-migrants can be noted. Other graphs display the change in vlaue of residential and non-residential buildings out of total number of buildings in each category. Due to the model dynamics, this can constantly change as buildings are either destroyed or become uninhabitable after an event, as they become rehabilitated or as they change use from residential to non-residential and vice-versa. While this visualization is not spatial, it enables the display of aggregated results (macro analysis) related to the entire study area over time and lets the user query the graphs with a mouse click.

Figure 5: Querying the dynamic charts by clicking on points in the graph representing the value of a variable at a certain point in time
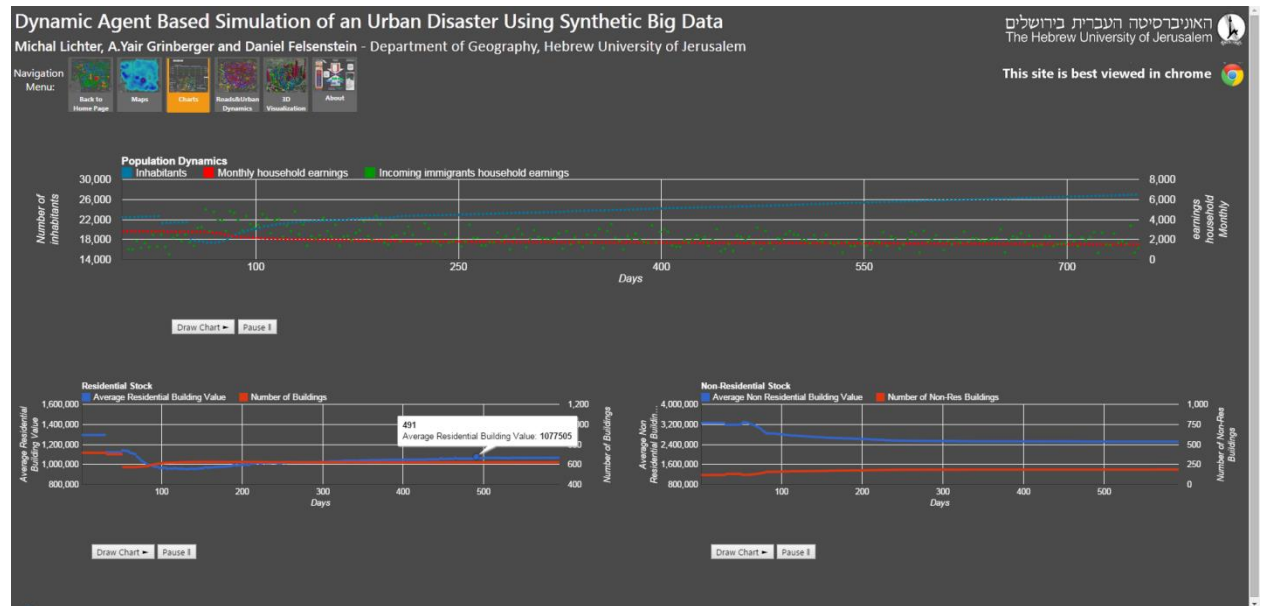
5.3 Roads and urban dynamics

This is a vector-based time lapse visualization which allows the animation of five different variables over time relating to change in the number of passangers along the road network in the study site (Figure 6). This change in traffic volume ultimately drives dynamic processes in the model through changing accessibility. Here too, the time lapse visualization is based on a 50 day interval over three years. The user can choose one variable to display with the road network: Land use, building value, vulnerability index, household income and mobility ratio. Since this is a vector based visualization, the user can query elements such as buildings and road segments in the map, using a mouse, and extract the properties of each element at each point in time. This visualization can be animated using the relevant buttons and can be manually manipulated using a time lapse slider.

Figure 6: Vector based 2D visualization of various variables over the road network
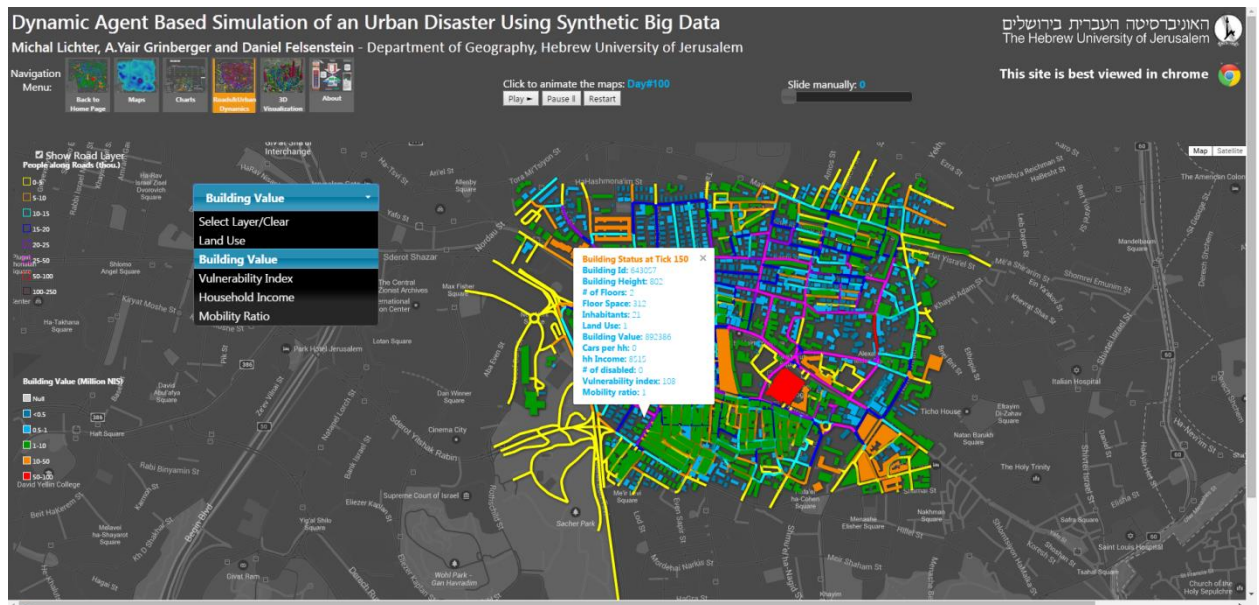
5.4 3D visualization

This visualization uses 3D visualization techniques to display the change in variables over time. We use the color of buildings to display change in each building land use and we use building height to display the change in building value, vulnerability index, household income and mobility ratio. Due to data volume constraints we limit the visualization to one year post the event with a 50 days time interval (Figure 7). This visualization also enables the user to familiarize the study site using 3D with Google Earth as the platform. Consequently, the user can rotate the scene and change the angle of presentation.

Figure 7: 3D visualization of various variables. Color represents the main land use of a building and height represents value of the variable.
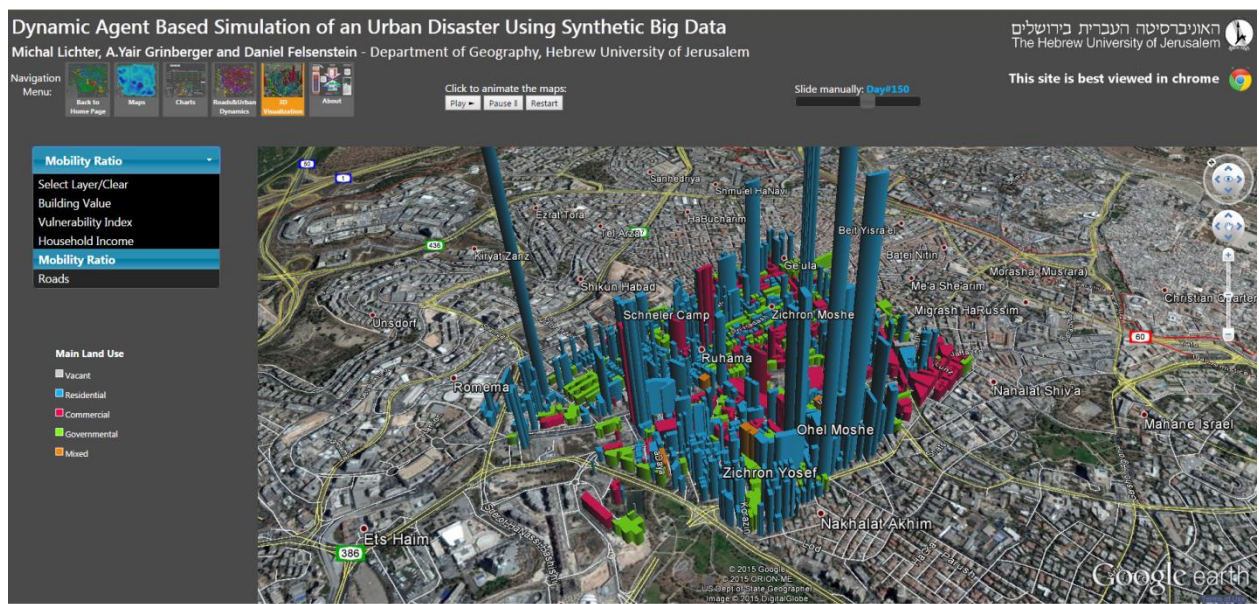
6. Design Steps

The multi-dimensional simulation outputs result in a voluminous database of spatial and temporal urban dynamics. The first challenge is to take these vast amounts of data and turn them into meaningful information. The second challenge is to design a visualization platform that will enable a comprehensible display of a large set of meaningful multi-dimensional results. We design a dedicated web-based application that allows interactive visualization and querying of the outputs in an intuitive and user-friendly fashion. (see http://ccg.huji.ac.il/AgentBasedUrbanDisaster/index.html). Using a web browser, the user can generate time animation visualizations in the form of maps and graphs without previous experience in GIS or spatial data handling. This requires a dedicated database design and construction of selected outputs to allow efficient and rapid application response and data extraction. We do this by using DB design that does not always follow strict DB design standards, but rather contains some flat tables to enable lateral data charting, displayed in pop-ups, graphs and charts.

6.1 Visualization Platforms

Our results are visualized using three main platforms (Figure 8):

(i)   Google Maps API is used as a 2D web-mapping platform.
(ii)   Google Earth API is used as a 3D display platform.
(iii)   Google Charts API is used as a non-spatial graphic visualization platform for aggregate results.

6.2 Data Formats

Each of the above mentioned platforms require different formats of input data, and sometimes accepts more than one input format interchangeably (Figure 8). The input data has to be designed so that it can be animated over both temporal and thematic dimensions.

(i)   Google Fusion Tables API - We use Google Fusion Tables API to feed spatial vector 2D layers into Google maps. Each feature in the layers contains time series of values for each variable. These are displayed using SQL queries generated in the background when an action button is clicked, when a slider button is dragged or when a feature is clicked upon.

(ii)   .Json data files – are used to create heat map visualizations using the 2D Google Maps API. Each time an action button is turned on or the slider is dragged back or forth, the time increment is changed, variable values are changed and the heat map draped over the study site changes accordingly.

(iii)   Graphs displayed using Google Charts API are based on a specific data format that feeds into this API. A JavaScript loop is written in order to generate the time lapse visualization initiated with a click of an action button.

(iv)   3D.kml files are generated in ArcScene to create the color and height symbology. Each file contains features representing the values of a

variable over a different time interval. An action button click or a drag of a slider changes the time interval of choice and calls for the appropriate .kml layer to be displayed and the previous layer to be turned off.

6.3 Middleware and Ancillary Functionalities

We use various JavaScript libraries and APIs in order to add middleware functionalities to the application. These middleware interact with the web-mapping platform to provide ancillary capabilities [29] such as time laps animation, selection of variable to show etc.

(i)   Action buttons– initiate an automatic looping time laps animation of a chosen variable in a map or graph in the different visualization platforms.

(ii)   Sliders – allow the user to manually slide through the visualization of a certain variable in the different visualization platforms.

(iii)   Selection menus – allow the user to browse through and choose a variable for display. A change in the choice of a variable also initiates a change in the displayed legends to fit the relevant variable.

Figure 8: Web visualization design roadmap
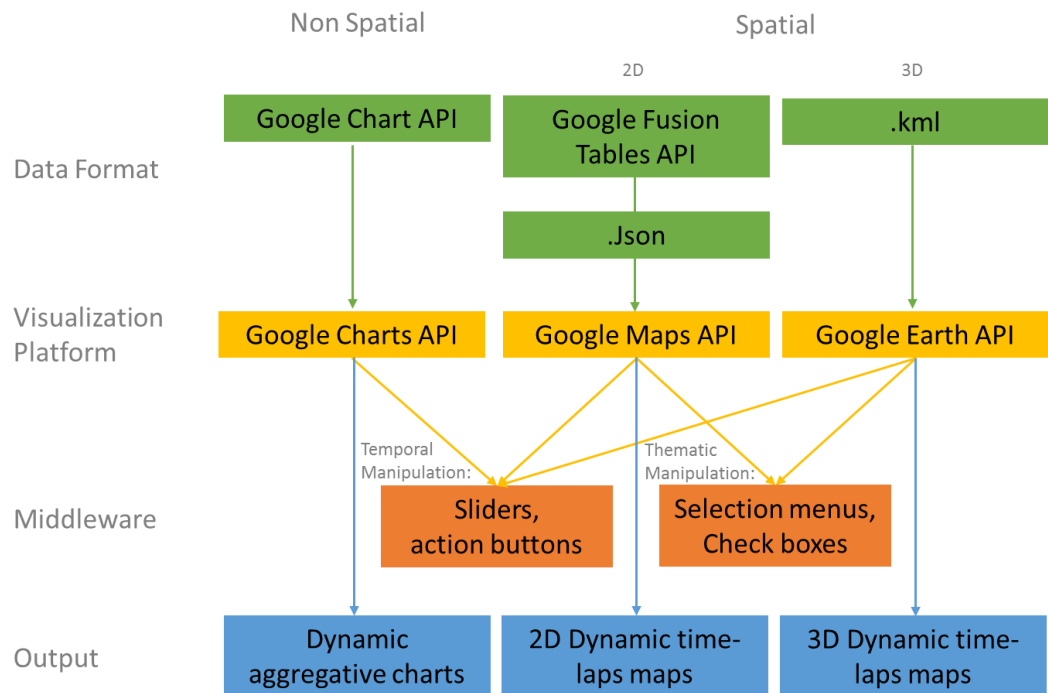
7. Conclusions

In terms of simulating outcomes, this paper has shown that diverse disaster situations result in very different outcomes. Over the long term, the city tends to recover from the earthquake and reaches equilibrium for key indicators over a period of 400-600 days. With the missile attack, things are rather different. The random, low-grade shocks erode re-organization capacity and the city never really recovers. This is also reflected at the micro level. The earthquake induces a process of dispersal and re-concentration of population and commercial activity. In contrast, the missile attacks cause residential and commercial clusters to decay as their capability to re-group is never allowed to materialize.

Just as these outcomes are very different, the methods of communicating them need to be delivered accordingly. The earthquake impacts need to be imparted to a population engaged in moving and re-adjusting post-disaster. In contrast, the missile outcomes need to be communicated to a population that stays put but gradually suffers from attrition. This implies that disaster management needs to move beyond providing engineering fixes and relate to wider process that differentiate across population groups affected by the disaster.

Improving accessibility to information is one route towards enahncing resilience to shocks. Along with the explosion of available information through enhanced computer power and techological progress, broader societal change also demands democratization of crisis management and increased citizen empowerment in the recovery process. The centralized, linear, top-down model of disaster management is slowly being augmented by a networked community-based approach [30]. This mode of management is grounded in data pooling and public input through crowdsourcing and is lubricated by resources such as OpenStreetMap and GeoCommons. In this respect, the internet acts as the great facilitator. It encourages open standards and simplified interfaces and generally makes information generation more transparent and democratic.

The web-based delivery of likely disaster outcomes not only encourages public participation in rebuilding and rejuvenation but also differentiates across the types of response required to withstand the shock. In our simulated cases, mitigating the effects of the earthquake point to the need for assisting recovery in new locations, encouraging personal mobility and removing regulatory contraints to the physical recovery of communities. For the missile attack case, a very different suite of interventions may be relevant. These relate to community preservation and stabilization, for example stemming the tide of out-migration and bolstering local social services.

Literature

1. Tate, E.; Burton, C. G.; Berry, M.; Emrich, C. T.; Cutter, S. L. Integrated Hazards Mapping Tool. *Trans. GIS* **2011**, *15*, 689–706.

2. Dransch, D.; Rotzoll, H.; Poser, K. The contribution of maps to the challenges of risk communication to the public. *Int. J. Digit. Earth* **2010**, *3*, 292–311.

3. Little, R. G.; Loggins, R. A.; Wallace, W. A. Building the Right Tool for the Job: Value of Stakeholder Involvement When Developing Decision-Support Technologies for Emergency Management. *Nat. Hazards Rev.* **2015**.

4. Hagemeier-Klose, M.; Wagner, K. Evaluation of flood hazard maps in print and web mapping services as information tools in flood risk communication. *Nat. Hazards Earth Syst. Sci.* **2009**, *9*, 563–574.

5. Kwan, M.-P.; Lee, J. Emergency response after 9/11: the potential of real-time 3D GIS for quick emergency response in micro-spatial environments. *Comput. Environ. Urban Syst.* **2005**, *29*, 93–113.

6. Roche, S.; Propeck-Zimmermann, E.; Mericskay, B. GeoWeb and crisis management: issues and perspectives of volunteered geographic information. *GeoJournal* **2011**, *78*, 21–40.

7. Chen, X.; Zhan, F. B. Agent-based modelling and simulation of urban evacuation: relative effectiveness of simultaneous and staged evacuation strategies. *J. Oper. Res. Soc.* **2006**, *59*, 25–33.

8. Crooks, A. T.; Wise, S. GIS and agent-based models for humanitarian assistance. *Comput. Environ. Urban Syst.* **2013**, *41*, 100–111.

9. Dawson, R. J.; Peppe, R.; Wang, M. An agent-based model for risk-based flood incident management. *Nat. Hazards* **2011**, *59*, 167–189.

10. Grinberger, A. Y.; Felsenstein, D. Bouncing back or bouncing forward? Simulating urban resilience. *Proc. ICE-Urban Des. Plan.* **2014**, *167*, 115–124.

11. Grinberger, A. Y.; Felsenstein, D.; Lichter, M. Simulating Urban Resilience: Disasters, Dynamics and (Synthetic) Data. In *Planning Support Systems and Smart Cities*; Geertman, S.; Stillwell, J.; Ferreira, J.; Goodspeed, R., Eds.; Springer, **2015** Forthcoming.

12. Macal, C. M.; North, M. J. Tutorial on Agent-based Modeling and Simulation. In *Proceedings of the 37th Conference on Winter Simulation*; WSC '05; Winter Simulation Conference: Orlando, Florida, 2005; pp. 2–15.

13. Salamon, A.; Katz, O.; Crouvi, O. Zones of required investigation for earthquake-related hazards in Jerusalem. *Nat. Hazards* **2009**, *53*, 375–406.

14. Linard, C.; Gilbert, M.; Tatem, A. J. Assessing the use of global land cover data for guiding large area population distribution modelling. *GeoJournal* **2010**, *76*, 525–538.

15. Reibel, M.; Bufalino, M. E. Street-weighted interpolation techniques for demographic count estimation in incompatible zone systems. *Environ. Plan. A* **2005**, *37*, 127–139.

16. Eicher, C. L.; Brewer, C. A. Dasymetric mapping and areal interpolation: Implementation and evaluation. *Cartogr. Geogr. Inf. Sci.* **2001**, *28*, 125–138.

17. Mennis, J. Generating Surface Models of Population Using Dasymetric Mapping. *Prof. Geogr.* **2003**, *55*, 31–42.

18. Beckman, R. J.; Baggerly, K. A.; McKay, M. D. Creating synthetic baseline populations. *Transp. Res. Part Policy Pract.* **1996**, *30*, 415–429.

19. Pritchard, D. R.; Miller, E. J. Advances in population synthesis: fitting many attributes per agent and fitting to household and person margins simultaneously. *Transportation* **2011**, *39*, 685–704.

20. Harper, G.; Mayhew, L. Using administrative data to count local populations. *Appl. Spat. Anal. Policy* **2012**, *5*, 97–122.

21. Harper, G.; Mayhew, L. Applications of population counts based on administrative data at local level. *Appl. Spat. Anal. Policy* **2012**, *5*, 183–209.

22. Beenstock, M.; Felsenstein, D.; Ben Zeev, N. Capital deepening and regional inequality: an empirical analysis. *Ann. Reg. Sci.* **2011**, 599–617.

23. Lichter, M.; Felsenstein, D. Assessing the costs of sea-level rise and extreme flooding at the local level: A GIS-based approach. *Ocean Coast. Manag.* **2012**, *59*, 47–62.

24. Crooks, A. T.; Castle, C. J. E. The Integration of Agent-Based Modelling and Geographical Information for Geospatial Simulation. In *Agent-Based Models of Geographical Systems*; Heppenstall, A. J.; Crooks, A. T.; See, L. M.; Batty, M., Eds.; Springer Netherlands, 2012; pp. 219–251.

25. Simon, H. A. A Behavioral Model of Rational Choice. *Q. J. Econ.* **1955**, *69*, 99–118.

26. Schelling, T. C. Dynamic models of segregation. *J. Math. Sociol.* **1971**, *1*, 143–186.

27. Dunn, C. E. Participatory GIS — a people's GIS? *Prog. Hum. Geogr.* **2007**, *31*, 616–637.

28. Elwood, S. Grassroots groups as stakeholders in spatial data infrastructures: challenges and opportunities for local data development and sharing. *Int. J. Geogr. Inf. Sci.* **2008**, *22*, 71–90.

29. Batty, M.; Hudson-Smith, A.; Milton, R.; Crooks, A. Map mashups, Web 2.0 and the GIS revolution. *Ann. GIS* **2010**, *16*, 1–13.

30. Kawasaki, A.; Berman, M. L.; Guan, W. The growing role of web-based geospatial technology in disaster response and support. *Disasters* **2013**, *37*, 201–221.